

Electromagnetic diffraction on a moving half-plane

A. Ciarkowski and B. Atamaniuk

Institute of Fundamental Technological Research

Polish Academy of Sciences

Abstract

A problem of electromagnetic (EM) plane wave diffraction on a moving half-plane in a homogeneous and isotropic medium is considered. It is shown, that unlike the stationary case, the shadow boundaries of the incident and reflected wave are not parallel to propagation directions of those waves. Other diffraction phenomena reported earlier for objects with moving edges, are also observed here.

1 Introduction

Studying wave scattering by objects in motion has a long history. This sort of EM field interaction with obstacles is characteristic of object recognition, space science and astronomy. Objects with sharp edges form a subclass of obstacles which are of both theoretical and practical interest. Phenomena associated with electromagnetic scattering on moving objects with edges, like Doppler shift of equiphase surfaces in the diffracted wave and angular shift of the location of its amplitude singularities, were observed in [1] and [2]. In more recent works ([3], [4], [5], [6]) new analytic and numerical results were obtained, which include alternative representation for the moving wedge solution, development of new numerical techniques, and extension of interacting fields to Gaussian beams.

A special problem in this area is that of EM diffraction by a moving half-plane. This problem is specially convenient for studying phenomena characteristic of a moving edge, because the location of shadow boundaries, and thus location of lit and shadow regions of geometrical optics (GO) field, can be inferred directly from the arguments of special functions defining the solution. Extra information on diffraction phenomena can be gained from studying high-frequency asymptotic expansion of the solution.

In this paper we assume that the field incident on the moving half-plane is a plane wave, and that the incidence direction is perpendicular to the half-plane edge. With the help of Lorentz transformation and the use of well known Sommerfeld solution obtained in stationary case the total field is found. This field is then asymptotically expanded and interpreted physically in terms of generated waves.

It is shown, that in addition to phenomena observed in the diffracted wave (comp. [2]), domains of existence of geometrical optics field are also modified.

2 Formulation of the problem

Assume that a perfectly conducting half-plane is in steady motion in a homogeneous and isotropic medium. We introduce two coordinate systems (x, y, z, t) and (x', y', z', t') , the first associated with the laboratory frame, and the other with the moving half-plane. To an observer in the primed system the half-plane is stationary and is described by $x' \leq 0$, $-\infty < y' < \infty$ and $z' = 0$. To an observer in the laboratory system, the primed system progresses along the positive x -axis with the constant velocity $\mathbf{v} = \hat{\mathbf{x}}v$. The two other axes, y' and z' , displace in space parallel to the corresponding axes y and z with the same velocity v .

Assume further that in the laboratory system, EM plane wave, varying in time as $\exp(-i\omega t)$, propagates in the direction perpendicular to the half-plane edge. Thus the problem is 2-dimensional and any EM field containing both electric and magnetic y -components can be decomposed into E - and H -parts with respect to y -axis, where those components are separated ([7]). In particular, a propagating plane wave can be represented as a sum of E -wave,

$$\mathbf{E}^i = [0, A_1, 0]e^{-ik(x \cos \theta + z \sin \theta + ct)}, \quad c\mathbf{B}^i = \frac{1}{ik}\nabla \times \mathbf{E}^i, \quad (1)$$

and H -wave,

$$c\mathbf{B}^i = [0, A_2, 0]e^{-ik(x \cos \theta + z \sin \theta + ct)}, \quad \mathbf{E}^i = -\frac{1}{ik}\nabla \times c\mathbf{B}. \quad (2)$$

Here, k and c are the wave number and the speed of light, respectively, $\theta \in (-\pi, \pi)$ is the incident angle measured from the positive x -axis to the direction from which the wave propagates, and A_i , $i = 1, 2$, are the amplitudes of the y components of the respective plane waves. (The ratio A_1/A_2 determines the polarization of the wave).

Thus a general, y -independent incident wave can be written down as

$$\begin{aligned} \mathbf{E}^i &= [-A_2 \sin \theta, A_1, A_2 \cos \theta]e^{-ik(x \cos \theta + z \sin \theta + ct)}, \\ c\mathbf{B}^i &= [A_1 \sin \theta, A_2, -A_1 \cos \theta]e^{-ik(x \cos \theta + z \sin \theta + ct)}, \end{aligned} \quad (3)$$

which is a sum of two plane waves of both types.

In what follows we find the field resulting from scattering of this wave on the moving half-plane and emphasize differences in its structure in comparison to the stationary case.

3 The scattered field

Our construction of the scattered field reduces to Lorentz transformation of the incident wave from the laboratory to the moving frame, employing there the well known Som-

merfeld solution for half-plane diffraction, and finally transformation of that solution back to the laboratory frame.

3.1 Lorentz transformation of the incident wave to the moving frame

Lorentz transformation of (3) leads to

$$\begin{aligned}\mathbf{E}^{i'} &= [-A'_2 \sin \theta', A'_1, A'_2 \cos \theta'] e^{-ik'(x' \cos \theta' + z' \sin \theta' + ct')}, \\ c\mathbf{B}^{i'} &= [A'_1 \sin \theta', A'_2, -A'_1 \cos \theta'] e^{-ik'(x' \cos \theta' + z' \sin \theta' + ct')},\end{aligned}\quad (4)$$

where

$$\gamma = (1 - \beta^2)^{-1/2}, \quad \beta = \frac{v}{c}, \quad (5)$$

$$A'_i = A_i \gamma (1 + \beta \cos \theta), \quad i = 1, 2,$$

$$\cos \theta' = \frac{\cos \theta + \beta}{1 + \beta \cos \theta}, \quad \sin \theta' = \frac{\sin \theta}{\gamma(1 + \beta \cos \theta)}, \quad (6)$$

and

$$k' = k\gamma(1 + \beta \cos \theta). \quad (7)$$

The last formula is a manifestation of Doppler effect: if the plane wave propagates in the direction opposite to \mathbf{v} , then $k' = k\sqrt{(1 + \beta)/(1 - \beta)} > k$, and hence $\omega' > \omega$. In this case the frequency in the moving frame is higher than that in the laboratory frame. Conversely, if the wave progresses in the direction coinciding with \mathbf{v} , then $k' = k\sqrt{(1 - \beta)/(1 + \beta)} < k$, and $\omega' < \omega$.

If the incident wave (3) propagates perpendicularly to \mathbf{v} , i.e. if $\theta = \pm\pi/2$, then by (6), $\theta' = \pm(\pi/2 - \arcsin \beta)$ and the direction of wave propagation in the primed system has a tendency to rotate in the direction opposite to that of \mathbf{v} .

3.2 The total field in the moving frame

The total field in the moving frame is obtained by the use of the well known Sommerfeld solution for stationary half-plane [8], together with the transformed incident wave (4). The corresponding solutions for each field type are as follows:

3.2.1 \mathbf{E} -field

In this case $\mathbf{E}' = \hat{\mathbf{y}}' E'_{y'}$, and the only component of the electric field is

$$E'_{y'} = A'_1 \frac{e^{-i\pi/4}}{\sqrt{\pi}} e^{ik'\rho'} [G(u') - G(v')] e^{-ik'ct'}. \quad (8)$$

Here,

$$G(a) = e^{-ia^2} \int_a^\infty e^{i\tau^2} d\tau, \quad (9)$$

$$u' = -\sqrt{2k'\rho'} \cos \frac{\phi' - \theta'}{2}, \quad v' = \sqrt{2k'\rho'} \cos \frac{\phi' + \theta'}{2}, \quad (10)$$

ρ' and θ' are cylindrical coordinates in the primed frame and the incident angle θ' is defined by (6).

The components of the magnetic induction are by (1) found to be

$$cB'_{x'} = A'_1 \frac{e^{-i\pi/4}}{\sqrt{\pi}} e^{ik'\rho'} \left\{ \sin \theta' [G(u') + G(v')] + i \sqrt{\frac{2}{k'\rho'}} \sin \frac{\phi'}{2} \cos \frac{\theta'}{2} \right\} e^{-ik'ct'} \quad (11)$$

and

$$cB'_{z'} = A'_1 \frac{e^{-i\pi/4}}{\sqrt{\pi}} e^{ik'\rho'} \left\{ \cos \theta' [G(u') - G(v')] - i \sqrt{\frac{2}{k'\rho'}} \cos \frac{\phi'}{2} \cos \frac{\theta'}{2} \right\} e^{-ik'ct'}. \quad (12)$$

3.2.2 H -field

Here, $c\mathbf{B}' = \hat{\mathbf{y}}' cB'_{y'}$, where

$$cB'_{y'} = A'_2 \frac{e^{-i\pi/4}}{\sqrt{\pi}} e^{ik'\rho'} [G(u') + G(v')] e^{-ik'ct'}. \quad (13)$$

The electric field is given by (comp. (2))

$$E'_{x'} = A'_2 \frac{e^{-i\pi/4}}{\sqrt{\pi}} e^{ik'\rho'} \left\{ \sin \theta' [G(u') - G(v')] - i \sqrt{\frac{2}{k'\rho'}} \cos \frac{\phi'}{2} \sin \frac{\theta'}{2} \right\} e^{-ik'ct'} \quad (14)$$

and

$$E'_{z'} = A'_2 \frac{e^{-i\pi/4}}{\sqrt{\pi}} e^{ik'\rho'} \left\{ \cos \theta' [G(u') + G(v')] - i \sqrt{\frac{2}{k'\rho'}} \sin \frac{\phi'}{2} \sin \frac{\theta'}{2} \right\} e^{-ik'ct'}. \quad (15)$$

3.3 The total field in the laboratory frame

Transformation of these fields back to the laboratory frame leads to the following expressions for both polarizations in the laboratory frame:

3.3.1 E -field

$$\mathbf{E}_\perp = A'_1 \gamma \hat{\mathbf{y}} \frac{e^{-i\pi/4}}{\sqrt{\pi}} e^{ik'\rho'} \left\{ (1 - \beta \cos \theta') [G(u') - G(v')] - i \sqrt{\frac{2}{k'\rho'}} \cos \frac{\phi'}{2} \cos \frac{\theta'}{2} \right\} e^{-ik'ct'}, \quad (16)$$

$$c\mathbf{B}_\parallel = A'_1 \hat{\mathbf{x}} \frac{e^{-i\pi/4}}{\sqrt{\pi}} e^{ik'\rho'} \left\{ \sin \theta' [G(u') + G(v')] + i \sqrt{\frac{2}{k'\rho'}} \sin \frac{\phi'}{2} \cos \frac{\theta'}{2} \right\} e^{-ik'ct'}, \quad (17)$$

$$c\mathbf{B}_\perp = A'_1 \gamma \hat{\mathbf{z}} \frac{e^{-i\pi/4}}{\sqrt{\pi}} e^{ik'\rho'} \left\{ (\beta - \cos \theta') [G(u') - G(v')] - i \sqrt{\frac{2}{k'\rho'}} \cos \frac{\phi'}{2} \cos \frac{\theta'}{2} \right\} e^{-ik'ct'}, \quad (18)$$

3.3.2 H -field

$$c\mathbf{B}_\perp = A'_2 \gamma \hat{\mathbf{y}} \frac{e^{-i\pi/4}}{\sqrt{\pi}} e^{ik'\rho'} \left\{ (1 - \beta \cos \theta') [G(u') + G(v')] + i \sqrt{\frac{2}{k'\rho'}} \sin \frac{\phi'}{2} \sin \frac{\theta'}{2} \right\} e^{-ik'ct'}, \quad (19)$$

$$\mathbf{E}_\parallel = A'_2 \hat{\mathbf{x}} \frac{e^{-i\pi/4}}{\sqrt{\pi}} e^{ik'\rho'} \left\{ \sin \theta' [G(u') - G(v')] - i \sqrt{\frac{2}{k'\rho'}} \cos \frac{\phi'}{2} \sin \frac{\theta'}{2} \right\} e^{-ik'ct'}, \quad (20)$$

$$\mathbf{E}_\perp = A'_2 \gamma \hat{\mathbf{z}} \frac{e^{-i\pi/4}}{\sqrt{\pi}} e^{ik'\rho'} \left\{ (\cos \theta' - \beta) [G(u') + G(v')] - i \sqrt{\frac{2}{k'\rho'}} \sin \frac{\phi'}{2} \sin \frac{\theta'}{2} \right\} e^{-ik'ct'}. \quad (21)$$

The total field is the sum of the component fields. For compactness, these fields are here given in terms of primed quantities.

3.4 Asymptotic representation of the total field

In an attempt to get insight into physical structure of the total field we asymptotically evaluate it as k' , or frequency, tends to infinity. The procedure reduces to the asymptotic expansion of the function $G(\cdot)$ in (16) through (21) as its argument tends to infinity. The result is ([7])

$$G(a) = H(-a) \sqrt{\pi} e^{i\frac{\pi}{4}} e^{-ia^2} + \frac{i}{2a} + O\left(\frac{1}{a^2}\right), \quad (22)$$

where $H(\cdot)$ is a Heaviside unit step function.

The term proportional to $H(-a)$ on the rhs of (22) is responsible for a geometrical optics field contribution, while the remainder contributes to the diffracted field. The lit and shadow domains of corresponding geometrical optics fields (here the incident and reflected waves) are specified by the sign of a , minus sign applies to the lit region, and plus sign to the shadow region. Those regions are separated by the shadow boundary, defined by $a = 0$.

Application of (22) to (16) through (21) yields the following asymptotic representation of the E - and H -field contributions to the total field in the laboratory frame:

E -field:

$$\begin{aligned} \mathbf{E}_\perp &\sim A_1 \hat{\mathbf{y}} (u^{GO-} + u_{e1}^d) \\ c\mathbf{B}_\parallel &\sim A_1 \hat{\mathbf{x}} (\sin \theta u^{GO+} + u_{e2}^d), \quad c\mathbf{B}_\perp \sim A_1 \hat{\mathbf{z}} (-\cos \theta u^{GO-} + u_{e3}^d), \end{aligned} \quad (23)$$

H -field:

$$\begin{aligned} c\mathbf{B}_\perp &\sim A_2 \hat{\mathbf{y}} (u^{GO+} + u_{h1}^d) \\ \mathbf{E}_\parallel &\sim A_2 \hat{\mathbf{x}} (-\sin \theta u^{GO-} + u_{h2}^d), \quad \mathbf{E}_\perp \sim A_2 \hat{\mathbf{z}} (\cos \theta u^{GO+} + u_{h3}^d). \end{aligned} \quad (24)$$

Here,

$$u^{GO\pm} = H(\epsilon^{i'}) e^{-ik(x \cos \theta + z \sin \theta) - i\omega t} \pm H(\epsilon^{r'}) e^{-ik(x \cos \theta - z \sin \theta) - i\omega t} \quad (25)$$

is a combination of the incident and the reflected plane wave, both waves vanishing in their shadow regions. The quantities

$$\begin{aligned} u_{e1}^d &= -\gamma f^+ g^+ h_1 s & u_{e2}^d &= \text{sign}(z) f^+ g^- h_2^+ s & u_{e3}^d &= -\gamma f^+ g^+ h_3 s \\ u_{h1}^d &= \text{sign}(\theta z) \gamma f^- g^- h_1 s & u_{h2}^d &= \text{sign}(\theta) f^- g^+ h_2^- s & u_{h3}^d &= -\text{sign}(\theta z) \gamma f^- g^- h_3 s \end{aligned} \quad (26)$$

represent the Cartesian components of the diffracted waves. The factors appearing in (26) are given by

$$f^\pm = \sqrt{\frac{(1 \pm \beta)(1 \pm \cos \theta)}{2ik}}, \quad (27)$$

$$g^\pm = \frac{\sqrt{r \pm (x - \beta ct)}}{r} \frac{1 + \beta \cos \theta}{(1 + \beta \cos \theta)(x - \beta ct) + (\cos \theta + \beta)r}, \quad (28)$$

$$h_1 = r + \beta(x - \beta ct) \quad h_2^\pm = r \pm (x - \beta ct) \quad h_3 = \beta r + x - \beta ct, \quad (29)$$

$$r = \sqrt{(x - \beta ct)^2 + (z/\gamma)^2}, \quad (30)$$

and

$$s = \exp [ik\gamma^2(1 + \beta \cos \theta)(r + \beta x - ct) - i\pi/4]. \quad (31)$$

The shadow indicators $\epsilon^{i(r)'}$ are discussed in the next section.

4 Phenomena specific to diffraction on a moving edge

Essential features in the field resulting from plane wave scattering by the moving half-plane are similar as in the stationary case, i.e. there are three different wave species appears in the solution: two plane waves – incident and reflected one, and the diffracted wave. Nevertheless, there are phenomena specific for moving edge diffraction. They are discussed below.

The shadow boundaries in the moving frame are defined by $u' = 0$ and $v' = 0$ for any ρ' , or equivalently by

$$\cos(\phi' \mp \theta') = -1, \quad \text{sign}(x') = -\text{sign}(\cos \theta'). \quad (32)$$

Here the upper (lower) sign applies to the incident (reflected) wave. By multiplying this by ρ' , squaring both sides and solving the resultant equation we find

$$\frac{z'}{x'} = \pm \tan \theta', \quad \text{sign}(x') = -\text{sign}(\cos \theta'). \quad (33)$$

This equation transforms in the laboratory frame into

$$\frac{z}{x - vt} = \pm \tan \theta \frac{1}{1 + \frac{\beta}{\cos \theta}}, \quad \text{sign}(x - vt) = -\text{sign}(\cos \theta + \beta). \quad (34)$$

For any time instant t , equations (34) describe semi-infinite straight lines in the (x, z) plane, with their starting points at the screen edge. If $0 < |\theta| < \pi/2$ then the effective angle defining the shadow boundary is less (in absolute value) then the incident angle θ , and if $\pi/2 < |\theta| < \pi$ that angle is greater than θ . In both cases there is a rotation of the shadow boundary towards the negative x half-axis as compared to the stationary case. Thus wave lit and shadow domains are modified with respect to stationary case. With changing t this line is shifted parallel in the x -direction.

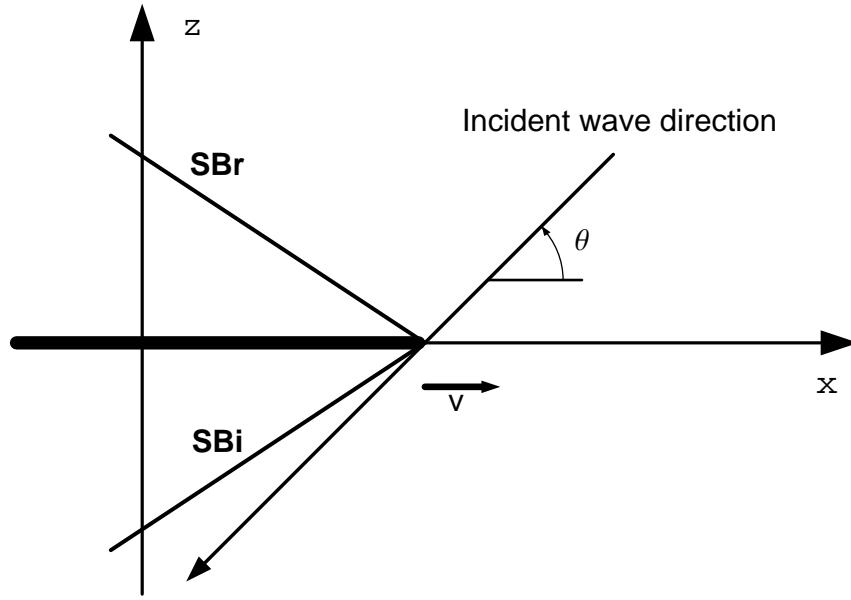


Fig.1 *Rotation of the shadow boundaries of the incident (SBi) and the reflected (SBr) waves for a moving half-plane.*

In the moving frame the diffracted wave can be physically interpreted as a cylindrical wave emanated from the half-plane edge. Its phase function is given by $k'\rho' - k'ct' - \pi/4$. Levels of constant phase in (x', z') space are coaxial, circular cylinders centered at $\rho' = 0$. In the laboratory frame it is given by

$$k\gamma^2(1 + \beta \cos \theta) \left[\sqrt{(x - \beta ct)^2 + (z/\gamma)^2} + \beta x - ct \right] - \pi/4, \quad (35)$$

(see (31)).

Equiphas surfaces in the laboratory frame are described by the equation

$$\sqrt{(x - \beta ct)^2 + (z/\gamma)^2} + \beta x - ct = C, \quad C = \text{const.} \quad (36)$$

It can be readily seen that for fixed C extremal values of z occur at $x = \beta\gamma^2 C$. Now (36) can be transformed into the form

$$(x + \beta\gamma^2 C)^2 + z^2 = (ct + \gamma^2 C)^2, \quad (37)$$

describing a circle of radius $ct + \gamma^2 C$, centered at $(-\beta\gamma^2 C, 0)$. The distance of the half-plane edge from the circle center is $\beta(ct + \gamma^2 C)$, i.e. it is β times smaller than its radius. Thus for $\beta < 1$ the edge is located always inside the circle, and it enters the circle if $\beta = 1$. As C increases, the circle centers are shifted along the x -axis backwards with respect to the direction of edge motion (see Fig.2)). This equation was first obtained in a different, but equivalent form in [1], where diffraction on a moving thin cylinder was examined.

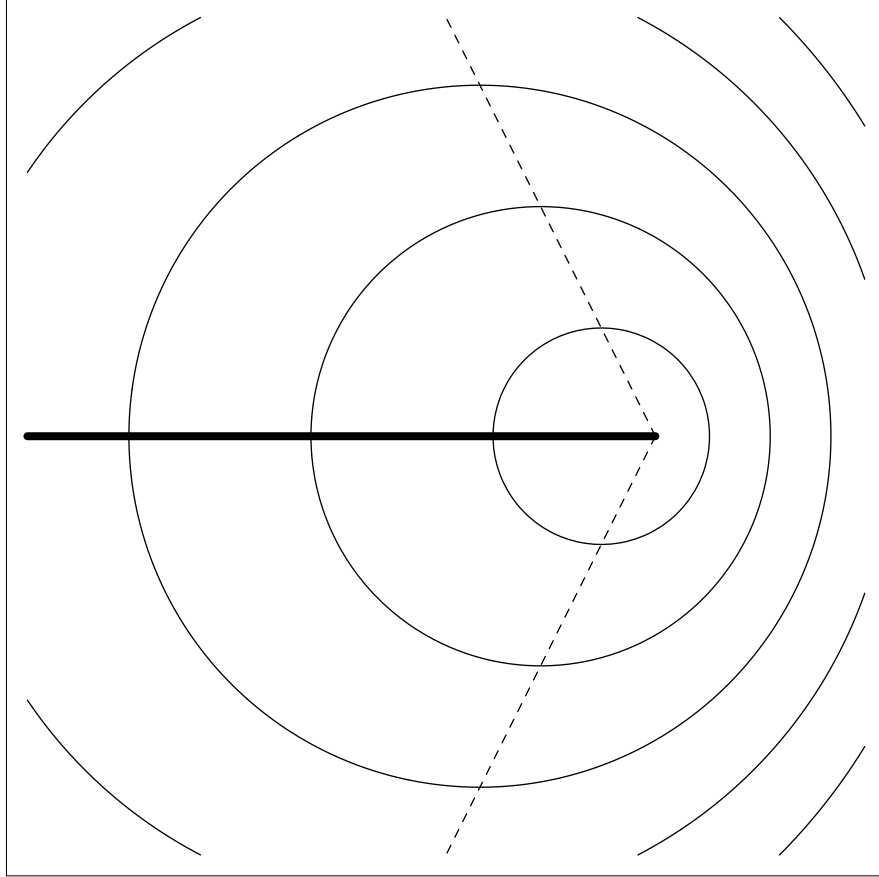


Fig.2 Equiphasic lines in the (x, z) plane. The dashed rays are drawn through the maximal and minimal values of z on them.

The loci of points corresponding to extremal values of z for different C are two semi-infinite straight lines

$$\frac{|z|}{x - vt} = -\frac{1}{\beta}, \quad (38)$$

(in primed coordinates they are given by $\beta + \cos \phi' = 0$). It is easy to see that along these lines $h_3 = 0$, and hence the z -components of the diffracted field also vanish on them. Additionally, z -component of phase velocity attains its maximal value c on these lines.

Singularities of the diffracted wave occur at all point where the denominator in g^\pm is zero, i.e. where

$$(1 + \beta \cos \theta)(x - \beta ct) + (\cos \theta + \beta)r = 0. \quad (39)$$

It then follows that the singularities appear on the straight lines

$$\frac{|z|}{x - \beta ct} = \frac{\sin \theta}{\cos \theta + \beta}, \quad \text{sign}(x - vt) = -\text{sign}(\cos \theta + \beta). \quad (40)$$

This fact was observed in [2] in the study of moving wedge diffraction. These lines are now recognized as coinciding with the shadow boundaries (34).

The fact that the equiphase surfaces in the diffracted wave are circles in the (x, z) plane is obvious — in a homogeneous medium EM signals excited from a point source propagate with the same velocity in all directions. Moreover, disturbances originated at the half-plane edge lag behind the edge as it is moving forward. This explains both the rotation of the shadow boundaries, as well as the shift of the equiphase surface centers backwards with respect to the edge. Above phenomena are similar to those which can be observed on water surface when disturbances are evoked on one side of a moving ship and at its bow.

5 Conclusions

In this work we examined 2D problem of EM plane wave diffraction on a moving half-plane. The classical Sommerfeld solution for a stationary problem and Lorentz transformation were used to obtain the solution in the laboratory frame. The field obtained is no longer time-harmonic, as it is in the stationary case. We expanded the exact solution asymptotically, and interpreted the result in physical terms. It appeared that for the half-plane displacement considered in this work the geometrical optics field has a similar form as in the stationary problem, except that the illuminated region of the incident wave and the shadow region in the case of the reflected wave increase in comparison to the stationary case. It was also shown that the surfaces of constant phase of the diffracted wave are circular cylinders, but they are not concentric, as they are in the stationary case. Even though these phenomena are most pronounced when β is close to 1, the results obtained are valid for arbitrarily β . If β is sufficiently small, these results can be simplified by replacing γ with its expansion for small argument, or even by putting $\gamma \approx 1$.

References

- [1] S.W. Lee, and R. Mittra: "Scattering of electromagnetic waves by a moving cylinder in free space", *Can. J. Phys.*, **45**, 9, 1967, pp. 2999-3007.
- [2] G.N. Tsandoulas: "Electromagnetic Diffraction by a Moving Wedge", *Radio Sci.*, **3**, 9, 1968, pp. 887-893.
- [3] P.De Cupis, G. Gerosa and G. Schettini: "Electromagnetic Scattering by an Object in Relativistic Translational Motion", *J. ElectroMagn. Waves Appl.*, **14**, 8, 2000, pp. 1037-1062.
- [4] P.De Cupis, G. Gerosa and G. Schettini: "Gaussian beam diffraction by uniformly moving targets", *Atti della Fondazione Gorgio Ronchi*, **LVI**, 4-5, 2001, pp. 799-811.
- [5] P.De Cupis, P. Burghignoli, G. Gerosa and M. Marziale: "Electromagnetic wave scattering by a perfectly conducting wedge in uniform translational motion", *J. ElectroMagn. Waves Appl.*, **16**, 8, 2002, pp. 345-364.
- [6] P.De Cupis: "Diffraction by a moving wedge: Comparison of analytic solution and numerical techniques", private communication.
- [7] M. Born and E. Wolf, *Principles of Optics*, Cambridge, 1964.
- [8] B. Noble, *Methods based on the Wiener-Hopf Technique*, London, Pergamon, 1958.